J. Inst. Eng. India Ser. C (July–September 2014) 95(3):273–289
DOI 10.1007/s40032-014-0131-3

CASE STUDY

Redesign of an Exhaust Gas Economiser Using Software

R. Balaji

Received: 8 April 2013 / Accepted: 10 July 2014 / Published online: 10 August 2014

Abstract Approaches to heat exchanger designs are numerous. Marine heat exchangers are usually single and they do not form part of a large network. Selections are generally based on the duties, area and the heat quantum. Over capacities and un-optimised designs could result. As an exercise to verify the choice, an existing heat exchanger on board of an operational ship was redesigned using computer software with thermodynamic data and standard geometric values. The formulae employed in the software were extracted and verified. The geometric data was used to develop the design drawings using SolidWorks®. Visualising the designs, the physical arrangement was improved. Comparisons and design improvements were made keeping the standard values in view. With the exercises, a method of developing an optimised physical design reducing the number of rating runs has been demonstrated.

Keywords Heat exchanger · Optimisation · Exhaust gas economiser · Design software

List of Symbols

A	Total surface area (m^2)
A_o	Total outside area, tube (approximated) (mm^2)
A_b	Area causing bypass streams (mm^2)
A_e	Smallest area for cross flow between baffles (mm^2)
A_{ee}	Area obtained from $S_e \cdot L_E$ (mm^2)
A_f	Area obtained as $A_f = D_i S$ (mm^2)
A_{gsb}	Area of gaps between shell and baffles (mm^2)
A_{gtb}	Total area of gaps between tubes and baffle holes (mm^2)
A_{sg}	Total area given by addition of A_{gsb} and A_{gtb} (mm^2)
A_t	Total area of tubes in the window section (mm^2)
A_{wt}	Flow area in window section including tubes in window (mm^2)
A_w	Flow area in window cross section (mm^2)
C	Constant obtained from Tables
Cp_c	Specific heat capacity, cold fluid (kJ/kg K)
Cp_h	Specific heat capacity, hot fluid (kJ/kg K)
D_i	Shell inside diameter (mm)
D_s	Shell outside diameter (mm)
D_{baf}	Baffle diameter (mm)
D_{bun}	Tube bundle diameter (mm)
D_{equi}	Equivalent diameter (mm)
$D_{noz\ in}$	Inlet nozzle diameter (mm)
F	LMTD correction factor
F_t	Fouling factor
G_s	Shell side mass flow velocity (kg/m^2 s)
G_t	Tube side mass flow velocity (kg/m^2 s)
H	Baffle cut height (mm)
K_e	Pressure drop factor
K_1	Constant based on number of tube passes
$LMTD$	Logarithmic mean temperature difference
L	Length of tubes (mm)
L_E	Sum of the shortest connections $(2e_1 + \sum e)$ (mm)
N_b	Number of baffles
N_t	Total number of tubes
Nu	Nusselt number
Nu_b	Nusselt number of the tube bundle at operating conditions
Nu_{cb}	Nusselt number calculated for tube bundle
Nu_{ib}	Nusselt number of ideal tube bundle

R. Balaji (✉)
Malaysian Maritime Academy (ALAM), Window Delivery 2051, P.O. Masjid Tanah, 78300 Melaka, Malaysia
e-mail: rajoobalaji@alam.edu.my

$Nu_{laminar}$	Nusselt number for laminar flow in a tube
Nu_s	Nusselt number, shell side
Nu_t	Nusselt number, tube side
$Nu_{turbulent}$	Nusselt number for turbulent flow in a tube
NTP	Number of tube passes
P	Temperature effectiveness
Pr	Prandtl number
Pr_t	Prandtl number of tube side fluid
Pr_w	Prandtl number at wall temperature
Q	Heat transferred (W)
R	Ratio of fluid capacities
R_{fi}	Fouling resistance inside (tube) (m^2 K/W)
R_{fo}	Fouling resistance outside (shell) (m^2 K/W)
R_B	Ratio A_b/A_e
R_G	Ratio n_w/N_t
R_L	Ratio A_{sg}/A_e
R_M	Ratio A_{gsb}/A_{sg}
R_S	Ratio n_s/n_{mr}
Re	Reynolds number
Re_e	Reynolds number in end cross flow section
Re_{s1}	Reynolds number for obtaining drag coefficients for turbulent and laminar flows
Re_t	Reynolds number for tube side fluid
$Re_{\Psi l}$	Reynolds number for a tube bundle
S	Baffle spacing (mm)
S_e	Baffle spacing in end channels (mm)
T_1	Shell side fluid inlet temperature (°C)
T_2	Shell side fluid outlet temperature (°C)
$T_{h,i}$	Hot fluid inlet temperature (°C)
$T_{h,o}$	Hot fluid outlet temperature (°C)
$T_{c,i}$	Cold fluid inlet temperature (°C)
$T_{c,o}$	Cold fluid outlet temperature (°C)
U	Overall heat transfer coefficient (W/m^2 K)
U_o	Overall heat transfer coefficient (approximated) (W/m^2 K)
U_w	Wetted perimeter (mm)
$\dot{V}$	Fluid flow rate (m^3/s)
a	Factor obtained from transverse pitch ratio (s_1/d_o)
b	Factor obtained from longitudinal pitch ratio (s_2/d_o)
d_b	Hole diameter in baffles (mm)
d_g	Equivalent diameter for window section (mm)
d_h	Hydraulic diameter (mm)
d_i	Tube inside diameter (mm)
d_n	Diameter of nozzle (mm)
d_o	Tube outside diameter (mm)
e	Shortest connection between adjacent tubes in the same row/adjacent row (mm)
e_1	Shortest connection between outermost tube and the shell (measured at the shell diameter parallel to baffle edge) (mm)
f_B	Bypass correction factor, shell side
$f_{Fanning}$	Fanning friction factor
f_L	Leakage correction factor, shell side
f_Z	Correction factor for change in physical properties, shell side
f_{alv}	Factor based on a, b and c
f_{atv}	Factor based on a and b
f_a	Tube arrangement factor
f_b	Bypass correction factor
f_g	Geometry correction factor
f_l	Leakage correction factor
f_n	Tube rows correction factor
f_p	Correction factor due to changes in physical properties near tube surfaces
f_w	Shell side flow correction factor
f_{zl}	Temperature correction factor (laminar flow)
f_{zt}	Temperature correction factor (Turbulent flow)
l'	Characteristic length (mm)
m_c	Mass flow of cold fluid (kg/s)
m_h	Mass flow of hot fluid (kg/s)
m_t	Mass flow in tube side (kg/s)
n	Exponent for Reynolds number
n_{pp}	Index based on number of tube passes and pitch arrangement
n_{mr}	Number of main resistances in cross flow between adjacent baffles (central section)
n_{mre}	Number of main resistances in end section
n_{mrw}	Number of effective main resistances in the window section
n_s	Number of pairs of sealing strips
n_w	Total number of tubes in lower and upper windows
r	Exponent as defined
s_1	Transverse tube pitch (mm)
s_2	Longitudinal tube pitch (mm)
t_1	Tube side fluid inlet temperature (°C)
t_2	Tube side fluid outlet temperature (°C)
w	Characteristic velocity (for Reynolds number) (m/s)
w_e	Velocity in the narrowest section of tube bundle (m/s)
w_{ee}	Velocity obtained from $\dot{V}/A_{ee}$ (m/s)
$w_{in\ noz}$	Velocity in the inlet nozzle (m/s)
w_n	Velocity in nozzle (m/s)
w_{nozzle}	Velocity in the nozzle section (m/s)
$w_{out\ noz}$	Velocity in the outlet nozzle (m/s)
w_p	Velocity in window section as defined (m/s)
w_t	Velocity of fluid flow in tubes (m/s)
w_z	Velocity in window section as defined (m/s)
α_i	Tube side heat transfer coefficient (W/m^2 K)
α_o	Shell side heat transfer coefficient (W/m^2 K)

η_{sm}	Dynamic viscosity (mean), shell side fluid (Pa s)
η_s	Dynamic viscosity, shell side fluid (Pa s)
η_t	Dynamic viscosity, tube side fluid (Pa s)
η_w	Dynamic viscosity of fluid at wall temperature (Pa s)
λ_s	Shell side thermal conductivity (W/m K)
λ_t	Tube side thermal conductivity (W/m K)
$\xi_{friction}$	Drag coefficient due to friction
ξ_{lam}	Drag coefficient (laminar flow)
ξ_{noz}	Drag coefficient for inlet or outlet nozzles
ξ_{stb}	Drag coefficient for shell side staggered tube bundle
$\xi_{tube\ in}$	Drag coefficient for tube side inlet nozzle
ξ_{tube}	Drag coefficient obtained after corrections
ξ_{turb}	Drag coefficient (turbulent flow)
ρ_{noz}	Density of fluid in the nozzle region (kg/m^3)
$\rho_{in\ noz}$	Density of fluid at inlet nozzle (kg/m^3)
$\rho_{out\ noz}$	Density of fluid at outlet nozzle (kg/m^3)
ρ_{sm}	Density (mean) of shell side fluid (kg/m^3)
ρ_s	Density of shell side fluid (kg/m^3)
ρ_t	Density of tube side fluid (kg/m^3)
$\Delta p_{in\ noz}$	Pressure drop in inlet nozzle (Pa)
Δp_{qe0}	Pressure drop in end sections without bypass & leakage streams (Pa)
Δp_{return}	Pressure drop approximated for nozzle entry/exit and flow (Pa)
Δp_{shell}	Pressure drop in shell side (Pa)
$\Delta p_{tube\ friction}$	Pressure drop in tubes due to friction (Pa)
Δp_{tube}	Pressure drop in the tubes (Pa)
Δp_{wlam}	Pressure drop due to laminar flow regime in window section (Pa)
$\Delta p_{w\ turb}$	Pressure drop due to turbulent flow regime in window section (Pa)
$\Delta p_{e\ in\ out}$	Pressure drop in inlet and outlet nozzles (Pa)
$\Delta p_{friction}$	Pressure drop in tube side due to friction (general equation) (Pa)
Δp_n	Pressure drop in nozzles (Pa)
$\Delta p_{out\ noz}$	Pressure drop in outlet nozzles (Pa)
Δp_{qo}	Pressure drop in central section without leakage and bypass streams (Pa)
Δp_q	Pressure drop in central section between adjacent baffles (Pa)
Δp_{qe}	Pressure drop in end section (Pa)
$\Delta p_{tube\ friction}$	Pressure drop due to tube friction (Pa)
Δp_w	Pressure drop in window section (Pa)
ΔT_{lm}	Logarithmic mean temperature difference (°C)
Φ	Viscosity Correction factor
α	Heat Transfer coefficient (W/m^2 K)
β	Constant for calculating bypass correction factor
γ	Central angle due to baffle cut degrees
λ	Thermal conductivity (W/m K)
v	Kinematic viscosity (m^2/s)
ξ	Drag coefficient
ρ	Density (kg/m^3)
Ψ	Void fraction factor

Introduction

Heat exchangers are an integral part of many marine engineering systems. Ships have heat exchangers for heating, cooling, evaporating and condensing processes. From technical point of view,classifications are based on the transfer process, constructional features, and flow arrangements as also on surface compactness etc. [1]. Heat exchangers may be further classified according to the passes, fluid states and intended duties etc. Of the many types, the shell and tube design, plate type and extended surface heat exchangers are regularly used in engine and Heating, Ventilation, Air Conditioning (HVAC) systems.

Shipboard heat exchangers are purposefully singular and are chosen for specific duties with few parameters such as maximum heat quantum and space availability. Commercially available exchangersare usually selected with little optimisation.Mostly, heat exchangers are designed with software and complex optimisation techniques. Optimisation of shell and tube design using non-linear programming has been demonstrated [2]. Optimisations with genetic algorithms [3, 4], simulated annealing [5] and various economics based approaches [6, 7] have also been demonstrated. A number of mechanical variables and thermal–hydraulic variables need to be optimised in these cases. Most of these approaches are complex and focus on solutions for processing industry. Using established constraints, reduction in thermal areas are obtainable within lesser number of rating runs [8]. For marine heat exchangers, simpler optimisation techniques using Lagrangian methods [9] can also be used by reducing the number of variables. The variables can be further reduced if their values are finalised rationally by using mathematical formulae.

While creating design populations, the choices are numerous which can be represented as an optimisation problem. The process is complex with many discrete decision variables, and obviously, choice of a vector would include numerous variables. If such variables are reduced, population for optimisation can be reduced. The choice of number of designs ($\bar{X}$) may be said to involve as many factors considered. Table 1 illustrates the generation of the design population and the rational reduction.

Table 1 Reducing design populations

Variable	Factor	Available	Considered for design exercise
x_1	Tube diameter	>10	2
x_2	Tube layout	2	1
x_3	Tube passes	5	1
	Total	**30**	**2**

$$\bar{X} = \langle x_1 \cdot x_2 \cdot x_3 \cdot x_4 \cdot x_5 \ldots x_n \rangle$$

In the example shown, only three factors for tube are considered. If options for other factors such as shell diameter (>10 choices available) and baffle cuts (minimum 3 choices within the range of 15–40 %), are included, the population will increase to 900. For shipboard systems, where parameters can be defined, these populations can be reduced by making rational choices. For example, tube lengths and shell diameters may be chosen keeping in mind the limited space available. In this study, an approach to reduce the variables using calculation software and engineering software was employed.

To verify the effectiveness of the approach, an exhaust gas economiser on an operational vessel was chosen and design data was obtained from the machinery manuals and drawings. On motor ships propelled by diesel engines, an economiser is a regular arrangement to recover some energy lost in the exhaust gases. Since some waste heat is recovered, this is referred to as an exhaust gas economiser. The water is pumped from the boiler steam drum to the economiser sections and returned. Saturated steam is generated in the boiler drum and drawn for consumption. For all practical purposes, the heat addition is for a single phase flow of feed water. An alternative to the existing economiser was developed redesigning the heat exchanger.

Geometric values were adopted from the drawings developed using SolidWorks® software.The values obtained from the equations were verified with the standards. Standard recommendations of Tubular Exchanger Manufacturers Association (TEMA) were referred to. The populations for design were thus reduced.Calculations were done and verified using MS Excel and MATLAB wares.

Methodologies

The steps followed confirm the basic design procedure suggested by Bell [10]. The approximations were computed for a shell and tube design with counter flow arrangement. The basic principles of iterations and stepwise calculations of software were verified following illustrative examples of Mukherjee [11]. The summary of the methodology steps is shown in Fig. 1.

The fundamental equation for heat exchange is

$$dA = dQ/U \cdot \Delta T \tag{1}$$

where dA is the elemental area required to transfer the heat, dQ is the heat at the location, U is the overall heat transfer coefficient and ΔT is the bulk temperature difference between the hot and cold streams. The integrated value of

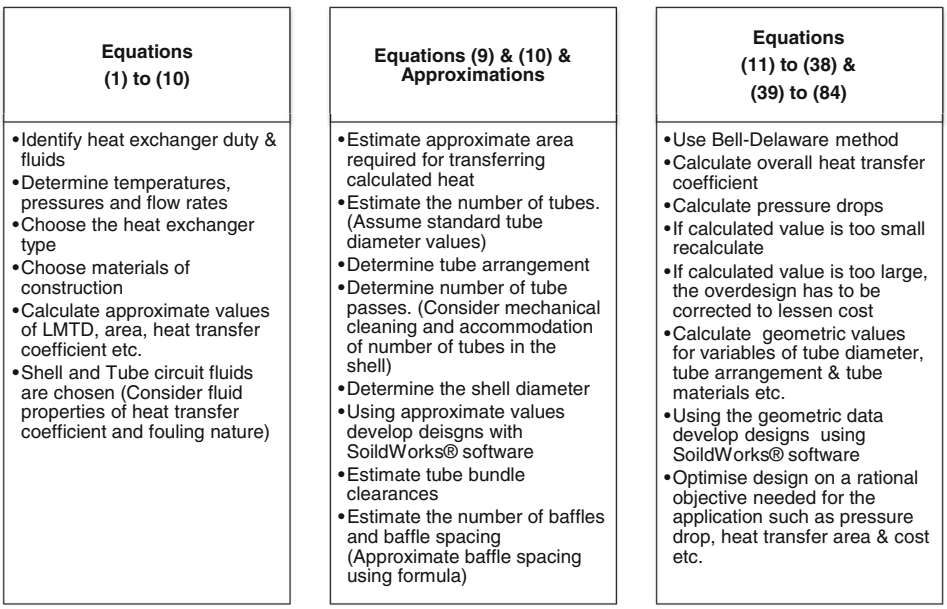

Fig. 1 Summary of methodology steps

A gives the total area of heat exchanger, provided the values of U, Q ΔT and are known.

$$A = Q/U \cdot \Delta T \tag{2}$$

Further modifying to suit the shell and heat exchanger design, Eq. (2) becomes,

$$Q = UAF\Delta T_{lm} \tag{3}$$

For initial estimation Q may be equalled as,

$$Q = U_o A_o F \Delta T_{lm} \tag{4}$$

where U_o and A_o are approximately computed values. For the heat balance, the heat absorbed by the cold stream must be equal to the heat given up by the hot stream.

$$Q = m_c \cdot C_{pc}(t_2 - t_1) = m_h \cdot C_{ph}(T_1 - T_2) \tag{5}$$

From these equations, the outlet temperatures of the process fluids are found. From the range of temperatures of the process fluids, the *LMTD* is calculated. The logarithmic mean temperature difference (*LMTD*), ΔT_{lm} and the correction F depend on the characteristics of the heat exchanger. The temperatures of the fluids change as they pass through the heat exchanger depending on the orientation of the flow. The basic flows assumed for the designs are concurrent or parallel flow and counter flow.

$$LMTD\ \Delta T_{lm} = \frac{(T_1 - t_2) - (T_2 - t_1)}{\ln\left[\frac{T_1 - t_2}{T_2 - t_1}\right]} \tag{6}$$

The correction factor F is applied for counter current heat exchangers depending on the number of tube and shell passes of the process fluids. Though the tube side fluid flow may be assumed to be unidirectional, the shell side flow is rather mixed due to the guided flow of the baffles. The correction factor, F depends on two factors, P and R.

P indicates the temperature effectiveness on the cold side and is the ratio of heat actually transferred to the heat which would have been transferred if the temperature of the cold fluid was raised to that of the inlet temperature of the cold fluid.

$$P = \frac{T_{c,o} - T_{c,i}}{T_{h,i} - T_{c,i}} \tag{7}$$

R is the ratio of the cold fluid capacity to that of the hot fluid capacity, also determined by the temperatures.

$$R = \frac{T_{h,i} - T_{h,o}}{T_{c,o} - T_{c,i}} \tag{8}$$

For various approximations at the initial stages of design, computed curves of F, P, R can be used. The curves are found in Tubular Exchange Manufacturers' Association (TEMA) [12]. For counter flow heat exchangers, the value of F must be close to unity. In all other cases, the values lying in the steep sections of the curve must be avoided to maintain the thermodynamic feasibility of the heat exchanger design.

Having approximated U_o, corrected *LMTD* and finalised Q, the outside area required for heat transfer and the number of tubes are calculated from,

$$A_o = N_t(\pi d_o)L \tag{9}$$

The shell size is selected to accommodate the length and tubes from the standard values. The next step is to calculate the overall heat transfer coefficient, U, to complete the iteration loop for approximations.

$$\frac{1}{U} = \frac{1}{\alpha_o} + \frac{1}{\alpha_i} \cdot \frac{d_o}{d_i} + \frac{d_o}{2\lambda} \ln\left(\frac{d_o}{d_i}\right) + R_{fo} + R_{fi} \tag{10}$$

The fouling resistances on the outside (shell side), R_{fo} and the inside (tube side) R_{fi} depend on the fluids and approximations can be applied from available data [13]. The thermal conductivity λ is tube material specific which is again assumed from material data. At this stage, many of the geometric data such as tube diameter, shell internal and external diameter etc. were approximated and calculations were done for a reasonable heat transfer coefficient. With such assumptions, approximate values of heat transfer coefficients and pressure drops were calculated. While calculating precise values, Bell-Delaware approaches [14, 15] were adopted. A similar approach projecting a compact formulation considering baffle leakage and bypass has been demonstrated by Serna and Jiménez [16]. The iterations for the present calculations are explained below.

Calculation of Tube-Side Heat Transfer Coefficient

For calculating heat transfer coefficients, similar methods can be employed, thereby reducing the number of steps. The heat transfer coefficient is calculated for the whole tube bundle. The relation to the maximum flow velocity between the tubes is considered [14]. The dimensionless Nusselt Number is derived from the general equation,

$$Nu = \frac{\alpha l'}{\lambda} \tag{11}$$

In the general equation, α is the heat transfer coefficient, l' is the characteristic length of the system and λ is the thermal conductivity.

The heat transfer coefficient for tube side, α_i is calculated from,

$$\alpha_i = \frac{\lambda_t}{d_h} Nu_t \tag{12}$$

To determine the Nusselt Number, the nature of the flow can be determined by calculating the Reynolds Number.

$$Re_t = \frac{\rho_t w_t d_h}{\eta_t} \tag{13}$$

A correction for the Nusselt Number may be applied, depending upon the fluid being liquid or gas.

For $Re_t > 10{,}000$, with turbulent flow, following equation is applied [15].

$$Nu_t = \frac{Re_t Pr_t \xi/8}{1 + 12.7\sqrt{\xi/8}(Pr_t^{2/3} - 1)}\left[1 + \left(\frac{d_h}{L}\right)^{2/3}\right] \tag{14}$$

This applies to a fully developed turbulent flow for $0.5 < Pr_t < 2{,}000$ and $3{,}000 < Re_t < 1{,}000{,}000$. The Friction Factor is obtained from $\xi = (0.78 ln\, Re_t - 1.5)^{-2}$.

Calculation of Shell-Side Heat Transfer Coefficient

For obtaining initial values, approximations were obtained based on relationship between Nusselt Number, Reynolds Number and Prandtl Number [17]. The general equations are as follows.

$$Nu = \frac{\alpha_o d_o}{\lambda_s} = CRe^n Pr^{1/3} \tag{15}$$

The constant C is obtained from tabulated values. This depends on the ratio of tube pitch to the tube outside diameter. The exponent n is also obtained from the tables. This value depends upon the tube arrangement being square or staggered. The Reynolds Number is found using the general formula involving density, dynamic viscosity, tube outside diameter and the velocity of flow over the tubes. The fluid velocity is obtained from dividing the volumetric flow on the shell side by the cross flow area. The calculation of the cross flow area is obtained from the following.

$$\begin{aligned} Cross\,flow\,area = {} & (Internal\,Dia.\,of\,shell) \\ & \cdot (Baffle\,Spacing) \\ & \cdot \frac{Clearance\,between\,tubes}{Tube\,Pitch} \end{aligned}$$

The Prandtl Number and values for other computations are computed for arithmetic average of the fluid temperatures at inlet and outlet. A correction is applied for the ideal heat transfer coefficient α_o to accommodate the various correction factors due to leakages etc. When the approximations come close to the assumed values of overall heat transfer coefficient after several considerations, a more precise value can be sought using the following steps.

Here again the shell side heat transfer coefficient is obtained from the Nusselt Number and the thermal conductivity.

$$\alpha_o = \frac{\lambda_s}{l'} Nu_s \tag{16}$$

The fluid stream on the shell side flows over half the circumference of the tube. The characteristic length of this stream flow l' is taken as $\pi\ d_o/2$. Then the equation becomes,

$$\alpha_o = \frac{\lambda_s}{(\pi/2)d_o} Nu_s \tag{17}$$

The calculation of the Nusselt Number for the shell side involves a number of steps and application of correction factors due to the flow variations on the shell side. Herein many geometric values need to be determined for the heat exchanger to get precise values.

The Nusselt Number is the mean value of the values over the tube bundle.

$$Nu_s = f_w Nu_b \tag{18}$$

The Nusselt Number for the bundle is calculated by applying corrections to the value for ideal tube bundle. One correction factor f_n is for the effect of the number of tube rows. The other correction factor f_p is for the change in the physical properties of the fluid's boundary layer flowing on the tube surface.

$$Nu_b = f_n f_p Nu_{ib} \tag{19}$$

The mean Nusselt Number for the bundle is obtained from the calculated value for the tube bundle. This value is again corrected by the arrangement factor f_a depending upon the tube arrangement being either in-line or staggered.

$$Nu_{ib} = f_a Nu_{cb} \tag{20}$$

The Nusselt Number for the ideal tube bundle is computed from Gnielinski equation involving the values due to laminar and turbulent flows over the bundle. The following steps are used.

$$Nu_{cb} = 0.3 + \sqrt{Nu_{laminar}^2 + Nu_{turbulent}^2} \tag{21}$$

$$Nu_{laminar} = 0.664\sqrt{Re_{\psi l}} \cdot \sqrt[3]{Pr} \tag{22}$$

$$Nu_{turbulent} = \frac{0.037 Re_{\psi l}^{0.8} Pr}{1 + 2.443 Re_{\psi l}^{-0.1}(Pr^{2/3} - 1)} \tag{23}$$

The Reynolds Number is calculated for mean velocity over the tube surface, characteristic length, void fraction and the kinematic viscosity. The mean velocity is computed from the fluid velocity in the void space and the channel width.

$$w = \frac{\dot{V}}{A_f} \tag{24}$$

V is the fluid flow rate and the area A_f is obtained as a product of inside diameter of the shell and the baffle spacing. So for $10 < Re_{\Psi l} < 1{,}000{,}000$,

$$Re_{\psi l} = \frac{w l'}{\psi v} \tag{25}$$

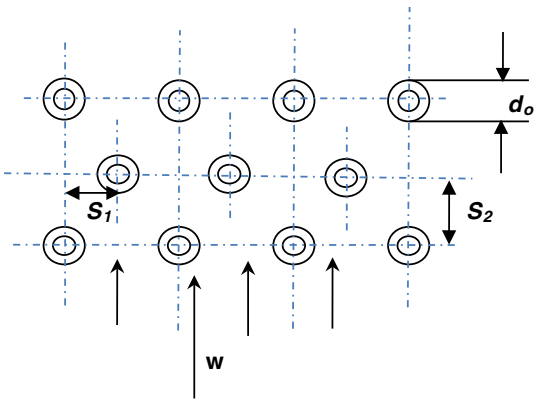

Fig. 2 Spacing in Staggered tube bundles

The void fraction is calculated from $\Psi = 1 - \pi/4ab$ if $b \leq 1$ or $-\pi/4a$ if $b < 1$, where $a = \frac{S_1}{d_o}$ and $b = \frac{S_2}{d_o}$. Figure 2 illustrates the spacing for staggered tube bundle arrangement from which the transverse pitch ratio *a,* and longitudinal pitch ratio *b* are obtained. The physical properties of the fluid are evaluated at a mean value of fluid inlet and exit temperatures of the fluid.

The calculation of the correction factors involves further systematic calculations.

Firstly, the arrangement factor is computed from the longitudinal pitch ratio.

$$f_a = 1 + \frac{2}{3b} \tag{26}$$

Secondly, f_n and f_p are ascertained. In a shell and tube exchanger with segmental baffles, the fluid flow between the segmental baffles differs from a cross flow across the tube bundle [15]. Hence f_n is neglected or may be assumed as 1.

The other correction factor f_p is dependent on the change in physical properties of the fluid flowing over the tube surface. This change is influenced by the nature of the heat exchange process. For cooling of gases, the correction is based on the ratio of temperatures and assumed to be 1 for the design. For heating of liquids with the ratio of Prandtl Numbers > 1, the correction factor is as follows.

$$f_p = \left(\frac{Pr}{Pr_w}\right)^{0.25} \tag{27}$$

Thirdly, the correction factor f_w is obtained as a product of correction factors for geometry, leakage and bypass and these are computed individually.

The geometry correction factor f_g is obtained from the following equation.

$$f_g = 1 - R_G + 0.524\, R_G^{0.32} \tag{28}$$

R_G is the ratio of number of tubes in the upper and lower window sections n_w to the total number of tubes N_t. Approximations can be applied from graphical values also.

The leakage correction factor f_l is calculated from the following equation.

$$f_l = 0.4\frac{A_{gtb}}{A_{sg}} + \left(1 - 0.4\frac{A_{gtb}}{A_{sg}}\right)\exp(-1.5R_L) \tag{29}$$

A_{sg} is the sum of all the gap areas. This is the total of all the gaps between the tubes and baffle holes and the gaps between the shell and the baffle, resulting in leakages and affecting the Nusselt Number.

$$A_{sg} = A_{gtb} + A_{gsb} \tag{30}$$

The area of gaps A_{gtb} between tubes and the baffle holes is computed from the following equation.

$$A_{gtb} = \left(N_t + \frac{n_w}{2}\right)\frac{\pi\left(d_b^2 - d_o^2\right)}{4} \tag{31}$$

The area of gap A_{gsb} between shell and the baffle is calculated from the following equation knowing the internal diameter of the shell D_i, the baffle diameter D_{baf} and the central angle of baffle cut [15].

$$A_{gsb} = \frac{\pi}{4}\left(D_i^2 - D_{baf}^2\right)\frac{360 - \gamma}{360} \tag{32}$$

The central angle of baffle cut is calculated in degrees [15, 18].

$$\gamma = 2\cos^{-1}\left(1 - \frac{2H}{D_{baf}}\right) \tag{33}$$

For computing the leakage correction factor, the last factor to be determined is R_L. This is the ratio of sum of the gap areas to the area for cross flow between two baffles.

$$R_L = \frac{A_{sg}}{A_e} \tag{34}$$

This area A_e, is measured at the row of tubes where the diameter of the shell is parallel to the edge of the windows. A_e is the product of the baffle spacing S and the sum of ligament gaps between tubes.

$$A_e = S \cdot L_E \tag{35}$$

The ligament gaps or the sum of the shortest connections between adjacent tubes and shortest connections between outermost tubes and the shell is given by $L_E = 2e_1 + \sum e$. All considered dimensions are illustrated in Fig. 3.

In this calculation of the leakage correction factor f_l, the gap area A_{gsb} must be maintained least, as this contributes to loss of heat transfer. The baffle spacing S is assumed to be constant. If the baffle spacing in the inlet/outlet regions and central regions are designed to be different, further correction has to be applied. The bypass correction factor f_b is then calculated. Here again the flow between the inner surface of the shell and the

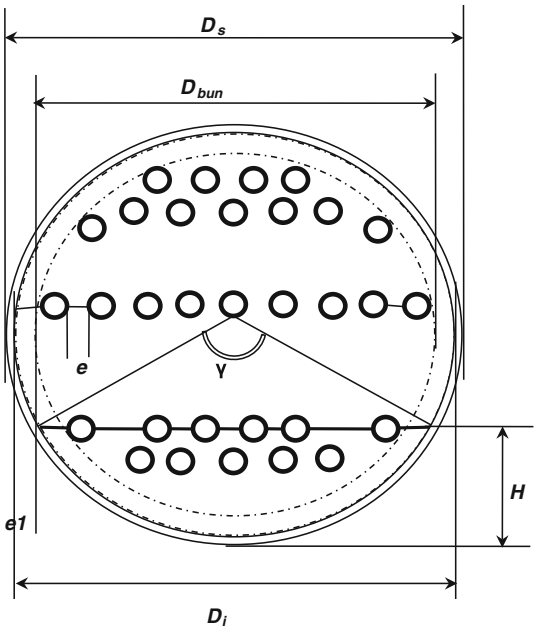

Fig. 3 Staggered tube layout

outermost row of tubes does not contribute to the heat transfer. In many shell and tube designs, sealing strips are provided to reduce this loss.

$$f_b = \exp\left[-\beta R_B\left(1 - \sqrt[3]{\frac{2n_s}{n_{mr}}}\right)\right] \tag{36}$$

A value of 1.5 or 1.35 is taken for the constant β depending on the flow being laminar or transient/turbulent. The number of pairs of sealing strips is given by n_s and n_{mr} represents the number of main resistances. The number of main resistances is for the fluid cross flow as it occurs between the upper and lower edges of adjacent baffles. The above equation holds good for the number of sealing strips being less than half the number of main resistances and where it is greater ($n_s > n_{mr}/2$), the value of f_b is taken as 1. Otherwise for computations, the ratio R_B needs to be calculated.

$$R_B = \frac{A_b}{A_e} \tag{37}$$

A_b is the cross sectional area resulting in the bypass and is obtained from the product of baffle spacing S and the computed diametrical clearance from internal diameter of the shell, the bundle diameter and the dimension e.

$$A_b = S(D_i - D_{bun} - e) \tag{38}$$

The value of f_b was assumed to be unity as no sealing strips were assumed to have been fitted.

Calculation of Tube-Side Pressure Drop

The general equation for computing the tube side pressure drop, assumed to be mainly due to friction, is as follows.

$$\Delta p_{tube\,f} = \xi_{friction} \cdot \frac{NTP \cdot L}{d_i} \cdot \frac{\rho_t w_t^2}{2} \tag{39}$$

The friction coefficient $\xi_{friction}$ can be obtained from equations or from graphs. The coefficient is dependent on the flow characteristic being laminar or turbulent as also the roughness of the tube. Approximate values for drag coefficient are obtained from graphs [15]. The pressure drops at nozzle entry/exit, flow etc., are termed as return losses and approximated using the following formula.

$$\Delta p_{return} = 4NTP \cdot \frac{G_t^2}{2\rho_t} \tag{40}$$

The mass flow velocity G_t is computed from the following general equation.

$$G_t = \frac{Tube\ side\ Mass\ Flow\ Rate}{Flow\ Area\ available/Tube\ Pass} \tag{41}$$

$$Flow\ Area\ available = \frac{N_t\,(Cross\ sectional\ area\ of\ onetube)}{NTP} \tag{42}$$

The addition of $\Delta p_{tube\,f}$ and Δp_{return} would give a good approximation of the tube side pressure drop. For precise values, extensive iterations are required, especially for gas flows in the tubes. The total pressure drop is the addition of drops in the inlet and outlet nozzles, inlet and outlet sections including any baffles and due tothe friction.

$$\Delta p_{tube} = \Delta p_n + \Delta p_{e\,in\,out} + \Delta p_{friction} \tag{43}$$

Tube Side Pressure Drop in the Nozzle Sections

$$\Delta p_n = \Delta p_{in\ noz} + \Delta p_{out\ noz} \tag{44}$$

The general equation for computing the pressure drop involves the drag coefficient, density and the velocity of the fluid in the nozzle. This is applied for inlet and outlet nozzles and the results are added up.

$$\Delta p_{noz} = \frac{\xi \Delta \rho}{2w_{nozzle}^2} \tag{45}$$

The fluid density variation due to temperature variation may also be applied if the temperature at nozzle entry can be approximated. For higher estimates of pumping power and costs, the densities and velocities may be assumed to be the same. The assumption of higher values will result in higher pressure drops and hence increased pumping power etc. Otherwise, the velocities at inlet and outlet nozzles are calculated separately using the respective densities, the

nozzle inside diameters and the tube side mass flow. The general equation is as follows.

$$w_{nozzle} = \frac{4m_t}{\pi \cdot D_{noz\,in}^2 \cdot \rho_{noz}} \tag{46}$$

Tube Side Pressure Drop in the Inlet, Outlet Sections

$$\Delta p_{e\,in\,out} = K_e \frac{\rho_t w_t^2}{2} \tag{47}$$

The pressure drop factor K_e is a constant depending upon the number of tube passes and varies from 0.9 for a straight tube/one pass to 1.6 for multiple passes in a U-tube configuration. Further, the velocity inside the tube and standard density are considered. The velocity is computed for one single tube by dividing the flow with the total number of tubes.

$$w_t = \frac{4m_t}{d_i^2 \cdot \rho_t \cdot N_t} \tag{48}$$

Tube Side Pressure Drop Due to Friction

The pressure drop due to friction is computed by applying a correction assuming uniform fouling of the tube surface.

$$\Delta p_{friction} = \Delta p_{tube\,friction} \cdot F_t \tag{49}$$

The pressure loss due to friction is obtained from the tube velocity, tube length, the number of passes, standard density, tube inside diameter and the drag coefficient due to friction.

$$\Delta p_{tube\,friction} = 2\xi_{tube} \frac{\rho_t \cdot w_t^2 \cdot NTP \cdot L}{d_i} \tag{50}$$

$$\xi_{tube} = \xi_{tube\,in} \cdot \Phi \cdot \Psi \tag{51}$$

The drag coefficient $\xi_{tube\ in}$ is obtained from the graphs for the specific Reynolds Number. For approximations, the value of Re_t can be applied. The Reynolds Number can be obtained from the general equation. The drag coefficient $\xi_{tube\ in}$ is corrected by applying the viscosity correction factor Φ and the convection correction factor Ψ to get the drag coefficient ξ_{tube}.

For approximating convective conditions, computations have to be done using the Prandtl Number, Grashof Number, the ratio of dynamic viscosity at mean temperature to that of wall temperature and other factors. For good approximations, the correction factors may be considered as unity. The Fouling Factor F_t is also assumed to be 1. Else the same is calculated by considering tube thickness and the tube outside diameter with more computations.

Calculation of Shell-Side Pressure Drop

For good approximations, the following formula is applied [9].

$$\Delta p_{shell} = \frac{2f_{Fanning} \cdot G_s^2 \cdot D_i(N_{baffle} + 1)}{\rho_s \cdot D_{equi}\left(\frac{\eta_s}{\eta_{sm}}\right)^{0.14}} \tag{52}$$

The factor $f_{Fanning}$ is referred to as the Fanning friction factor. The mass flow velocity G_s is calculated similar to the tube side equation but considering the mass flow and cross flow area on the shell side.

$$G_s = \frac{Shell\,side\,Mass\,Flow\,Rate}{Cross\,flow\,Area} \tag{53}$$

$$Cross\,flow\,Area = D_i \cdot S\left(\frac{Tube\,Clearance\,(e)}{Tube\,Pitch}\right) \tag{54}$$

The calculation of equivalent diameter D_{equi} involves the tube outside diameter, tube pitch, and a constant based on the tube arrangement. The estimated values of constant for square or staggered arrangements are obtained from pre calculated tabulations.

A closer pressure drop for the shell side is obtained by considering the drops in cross flow (central and end sections), window and the nozzle sections as developed in the Delaware Method. The comprehensive equation for the total shell side pressure drop is as follows. Figure 4 shows the regions of the pressure drops in the shell.

$$\Delta p_{shell} = (N_b - 1)\Delta p_q + 2\Delta p_{qe} + N_b \Delta p_w + \Delta p_n \tag{55}$$

Shell Side Pressure Drop in Central Section

The calculations of each pressure drop follow several steps. The steps for calculating each pressure drop is given in a progressive manner. Firstly, the pressure drop in the central section lying between two adjacent baffles is calculated. The upper and lower edges of the baffle cuts are treated as the boundaries for this section.

$$\Delta p_q = \Delta p_{qo} f_L f_B \tag{56}$$

In the above equation, Δp_{qo} represents the pressure drop when the flow occurs with no leakage and bypass effects.

$$\Delta p_{qo} = \xi_{stb} \cdot n_{mr} \cdot \frac{\rho_s w_e^2}{2} \tag{57}$$

The characteristic velocity w_e is given by,

$$w_e = \frac{\dot{V}}{A_e} \tag{58}$$

This is the mean velocity measured at a tube row nearest to or at the shell diameter parallel to the baffle cut edges. $\dot{V}$ is the volumetric flow in the shell circuit.

The drag coefficient for the tube bundle ξ_{stb} for a staggered tube arrangement is computed from the following equations.

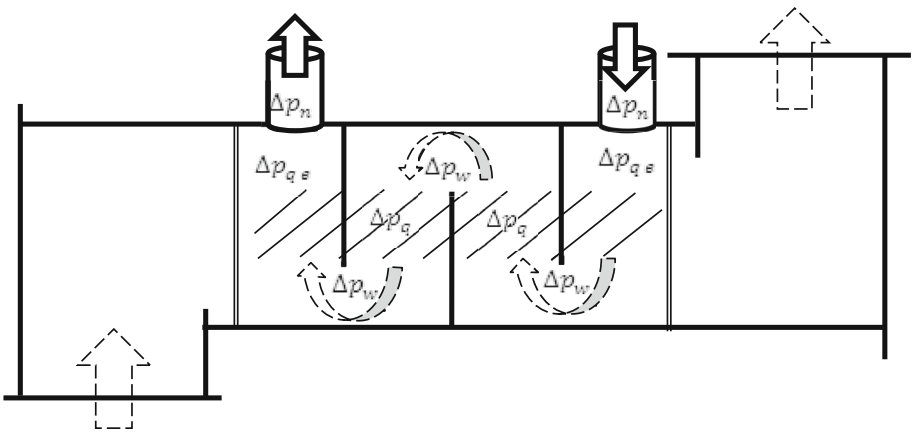

Fig. 4 Shell side pressure drop regions

$$\xi_{stb} = \xi_{lam} \cdot f_{zl} + \xi_{turb} \cdot f_{zt} \left[1 - exp\left(-\frac{Re_{s1} + 200}{1000}\right)\right] \tag{59}$$

where the drag coefficient due to laminar flow,

$$\xi_{lam} = \frac{f_{alv}}{Re_{s1}} \tag{60}$$

where,

$$f_{alv} = \frac{280\pi\left[\left(b^{0.5} - 0.6\right)^2 + 0.75\right]}{(4ab - \pi)a^{1.6}} \tag{61}$$

The above equation is applicable for $b \geq 0.5\sqrt{2a+1}$ and for $b < 0.5\sqrt{2a+1}$. In the denominator, instead of the transverse pitch ratio a, the diagonal pitch ratio $c^{1.6}$ is substituted. The diagonal pitch ratio $c = \left((a/2)^2 + b^2\right)^{0.5}$.

The drag coefficient for turbulent flow is then obtained.

$$\xi_{turb} = \frac{f_{atv}}{(Re_{s1})^{0.25}} \tag{62}$$

f_{atv} is a factor based on the transverse and longitudinal pitch ratios.

$$f_{atv} = 2.5 + \left(\frac{1.2}{(a - 0.85)^{1.08}}\right) + 0.4\left(\frac{b}{a} - 1\right)^3 \tag{63}$$

Reynolds Number Re_{s1} is computed using the characteristic velocity and the mean dynamic viscosity.

$$Re_{s1} = \frac{w_e d_o \rho_{sm}}{\eta_{sm}} \tag{64}$$

The correction factors for the drag coefficients f_{zl} and f_{zt} are obtained using the Reynolds Number, dynamic viscosities at mean and wall temperatures and the pitch ratios.

$$f_{zl} = \left(\frac{\eta_w}{\eta_{sm}}\right)^{\frac{0.57}{\left[\left(\frac{4ab}{\pi} - 1\right)Re_{s1}\right]^{0.25}}} \tag{65}$$

$$f_{zt} = \left(\frac{\eta_w}{\eta_{sm}}\right)^{0.14} \tag{66}$$

The dynamic viscosity and density are calculated for the mean fluid temperature in the shell circuit.The leakage and bypass correction factors f_L and f_B specific for tube bundle pressure drops are obtained from following steps.

$$f_L = exp\left[-1.33(1 + R_M)R_L^r\right] \tag{67}$$

The factor r is given by $[-0.15\ (1 + R_M) + 0.8]$, where $R_M = \frac{A_{gsb}}{A_{sg}}$. The sum of all gaps A_{sg} and areas of all gaps between tubes and holes A_{gsb} are as calculated earlier for computing the heat transfer coefficient.

The bypass corrections factor f_B is computed from the similar equation for computing heat transfer coefficient but with different considerations.

$$f_B = exp\left[-\beta R_B\left(1 - \sqrt[3]{2R_S}\right)\right] \tag{68}$$

The equation is valid for $R_S < \frac{1}{2}$. Here, the constant $\beta = 4.5$ (for laminar flow <100) and 3.7 for transition and turbulent flows ($Re \geq 100$). The ratios are computed as follows.

$$R_B = \frac{A_b}{A_e} \tag{69}$$

$$R_S = \frac{n_s}{n_{mr}} \tag{70}$$

If no sealing strips are used in the design, R_S works to zero. These steps help in computing the pressure drop Δp_q in the central cross flow section.

Shell Side Pressure Drop in End Sections

The next calculation is for the pressure drop in the end cross flow sections. The end cross flow section is identified as the region between the tube sheet and the immediate baffle. Figure 5 illustrates the path of the leakage streams in the cross flow sections.

The inlet section does not have a preceding leakage stream and the outlet section does not have a succeeding stream as in the central cross flow sections. Ignoring this,

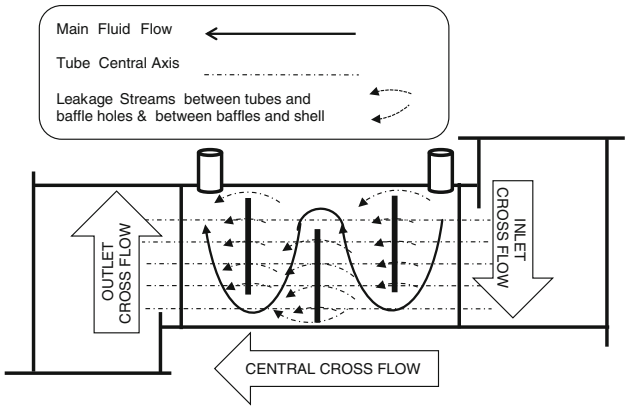

Fig. 5 Path of leakage streams in cross flow sections (shell side)

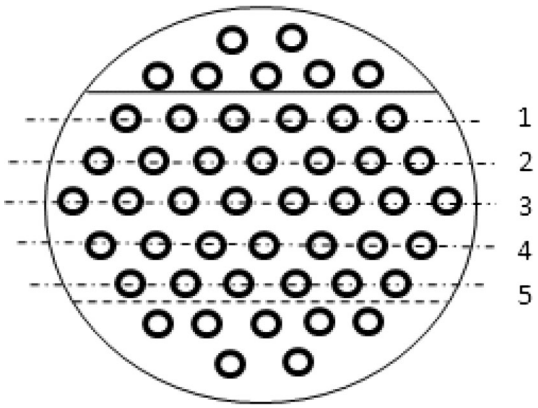

Fig. 6 Staggered tube arrangements: calculation of main resistances

the pressure drop for the end cross flow section is calculated. Again, if the bypass streams are non-existent then,

$$\Delta p_{qe} = \Delta p_{qe0} \cdot f_B \tag{71}$$

When the baffle spacing in the central section S and S_e in the end sections are not equal, the equation similar to pressure drop in central section is applied.

$$\Delta p_{qe0} = \xi_{stb} \cdot n_{mre} \cdot \frac{\rho_s w_{ee}^2}{2} \tag{72}$$

The drag coefficient is as calculated earlier but for a different Reynolds Number as computed below for the end zone. In other related computations, the values have to be related to this Reynolds Number for the end section.

$$Re_e = Re_{s1} \cdot \frac{S}{S_e} \tag{73}$$

The number of main resistances in the end section will differ from that of the resistances in the main section. The resistances are counted from the end view sketch of the tube arrangement. Figure 6 shows a typical view for staggered tube arrangement with five main resistances (exemplar)for the central cross flow sections.

The velocity in the end section is obtained from the following equation.

$$w_{ee} = \frac{\dot{V}}{A_{ee}} = w_e \frac{S}{S_e} \tag{74}$$

Shell Side Pressure Drop in Window Section

The window section pressure drop Δp_w is calculated next.

$$\Delta p_w = \sqrt{\Delta p_{w\ lam}^2 + \Delta p_{w\ turb}^2 f_z f_L} \tag{75}$$

$$\Delta p_{w\,lam} = \left[\frac{56}{\left(\frac{w_z \rho_s e}{\eta_{sm}}\right)} n_{mrw} + \frac{52}{\left(\frac{d_g w_z \rho_s}{\eta_{sm}}\right)} \left(\frac{S}{d_g}\right) + 2\right] \left(\frac{\rho_s w_z^2}{2}\right) \tag{76}$$

$$\Delta p_{w\ turb} = (0.6 n_{mrw} + 2) \left(\frac{\rho_s w_z^2}{2}\right) \tag{77}$$

The number of mean resistances n_{mrw} is obtained from $0.8H/s_2$. The equivalent diameter d_g for the flow section is obtained from

$$d_g = \frac{4A_w}{U_w} \tag{78}$$

The cross sectional flow area A_w and wetted perimeter in the section U_w are obtained from the following steps.

$$A_w = A_{wt} - A_t \tag{79}$$

The cross sectional area A_{wt} is the total area of section including the area of the tubes in the window.

$$A_{wt} = \frac{\pi}{4} D_i^2 \left(\frac{\gamma}{360}\right) - \frac{(D_{baf} - 2H) D_{baf}}{4} \cdot \sin\left(\frac{\gamma}{2}\right) \tag{80}$$

The area of the window tubes A_t will be the product of the outside area of a single tube and the number of tubes in the upper and lower window sections.

The wetted perimeter is calculated thus.

$$U_w = \pi D_i \left(\frac{\gamma}{360}\right) + \pi d_o \left(\frac{n_w}{2}\right) \tag{81}$$

The characteristic velocity for the window section w_z is calculated thus.

$$w_z = \sqrt{(w_e w_p)} \tag{82}$$

where $w_p = V/A_w$.

The temperature correction factor f_z would be chosen according to laminar or turbulent flow characteristics affecting the physical properties. This is determined by the value of the Reynolds Number.

The last pressure drop in the inlet and outlet nozzles to be calculated is Δp_n. The nozzle diameters are designed to be equal in diameter and the pressure drop is also assumed

to be same in each and will be cumulatively twice the calculated drop.

$$\Delta p_n = \xi_{noz} \frac{\rho_s w_n^2}{2} \tag{83}$$

The drag coefficient ξ_{noz} is assumed to be unity and the characteristic velocity is calculated from the volume flow and the nozzle area.

$$w_n = \frac{\dot{V}}{\frac{\pi}{4} d_n^2} \tag{84}$$

While approximating the baffle spacing, formula $74\, d_o^{0.75}$ may be employed. The number of baffles can be approximated using formula $(L/S) - 1$ equal to the number of baffles.

The above approaches including calculation of approximate values are comprehensively shown.

Results and Discussions

Design Considerations and Calculations

Referring to the steps given in Fig. 1, the heat duty was computed using Eq. (5) while the flow rates and temperatures were adopted from the ship's data. The significant calculation steps are summarised in Fig. 7 and values obtained using other equations are tabulated in "Appendix" section. The geometric dimensions extracted from the software and used for computations are shown in the columns of Tables 6 and 7.

Keeping the area as the objective for optimisation, two designs with different tube diameter were developed. The chosen tube diameter of 50 mm suited well for the sizing. The limiting factor was the size of the final design which was dependent on the tube length. With the chosen tube

Table 2 Primary data

Item	Tube side	Shell side
Fluid	Flue gas	Water
Flow rate	218,900 kg/h	25 m^3/h
Inlet temperature	250 °C	50 °C
Operating pressure	150,000 Pa, (abs)	1,000,000 Pa (abs)

Table 3 Data calculated for new design

	Tube side	Shell side
Mass flow	218,900 kg/h	23,938 kg/h
Inlet temperature	250 °C	158.5 °C
Outlet temperature	202.1 °C	165 °C
Mean temperature	226 °C	107.5 °C
Density	1.053 kg/m^3	957.5 kg/m^3
Specific heat capacity	1,103 J/kg K	4,204 J/kg K
Thermal conductivity	0.03846 W/m K	0.6861 W/m K
Dynamic viscosity	0.02498 mPa s	0.2635 mPa s
Velocity	31.08 m/s	0.02412 m/s

Table 4 Thermal data: shell and tube design

Parameter	
Heat duty	3,215 kW
Thermal conductivity, tube wall	52 W/m K
Heat transfer coefficient (inside)	109.4 W/m^2 K
Heat transfer coefficient (outside)	692.1 W/m^2 K
LMTD correction factor	0.997
LMTD	115.3 °C
Overall heat transfer coefficient	72.56 W/m^2 K

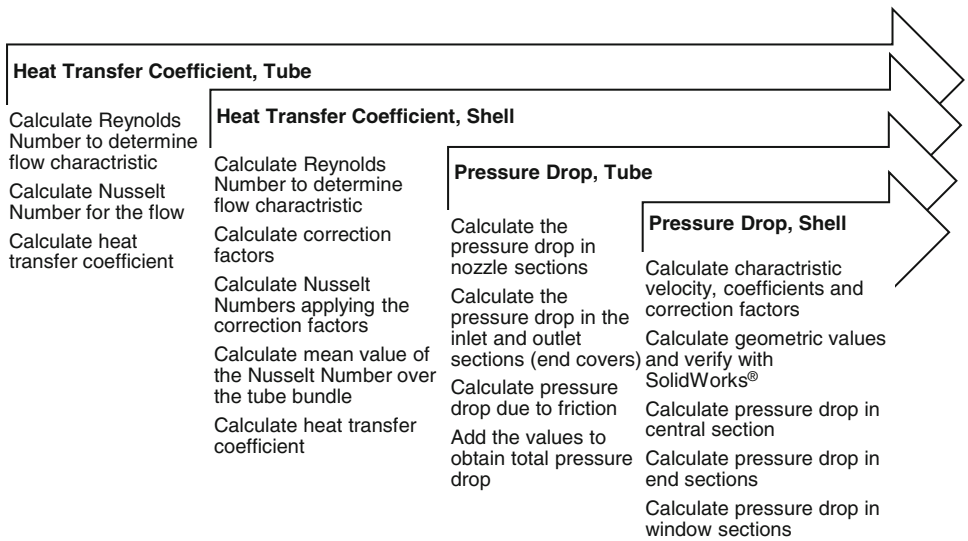

Fig. 7 Summary of calculation steps

diameter in staggered arrangement, the final area worked to 444.1 m^2 (overdesign 4.43 %). The number of tubes also was higher at 1,285. This design was improved to the current count of 1,099 by increasing the tube length resulting in a reduced area to 414.3 m^2 (overdesign 7.5 %).

For further validation of the geometric design, two physical values were changed and calculations were done. Firstly, one baffle was removed and pressure drops computed. The obtained values were within limits. Secondly, the tube pitch was reduced to 1.25 d_o (62.5 mm) and the tube bundle diameter was calculated using the following equation [19].

$$D_{bun} = d_o(N_t/K_1)^{\frac{1}{n_{pp}}} \quad (85)$$

The exercise was to check if this could reduce the area and hence the overall sizing. Furthermore, tube bundle diameter affects both heat transfer coefficient and pressure drops but has greater significance if sealing strips are used. Since the design had no sealing strips, reduction in area was tried varying this parameter.

Table 5 Geometric data comparison

	New design	Existing design
Number of tubes	1,099	160 finned tubes
Tube Material	Steel	Steel
Tube dimensions	50 × 1.8 × 2,400 mm	38.1 × 3.5 × 2,770 mm
Tube pitch	Triangular 21 × 60°	
Inlet nozzle diameter	2,020 mm (tube side)	1,883 mm (gas side)
Outlet nozzle diameter	2,020 mm (tube side)	1,883 mm (gas side)
Inlet nozzle diameter	140 mm (shell side)	80 mm (water side)
Outlet nozzle diameter	140 mm (shell side)	80 mm (water side)
Shell	2,400 × 20 mm	diameter × thickness
Shell dimensions	6,500 × 2,400 mm	3,602 × 2,200 × 2,994 mm
Number of baffles	3	na
Baffle pitch	472 mm	
Area required	385.4 m^2	
Area desired in design	414.3 m^2	536 m^2
Area overdesign	7.5 %	
Pressure drop (tube side)	1,488 Pa	<100,000 Pa (designed)
Pressure drop (shell side)	304.6 Pa	

When the reduced value of tube bundle diameter 2,241.3 mm was applied to the software drawing, the ligament (free) area in the end plates was weakened though not much variation in heat transfer coefficient and pressure drops were seen. The tube bundle diameter was restored to 2,305 mm. With such approaches, no further reduction in area could be achieved. With the finalised design, gas velocity was slightly increased over targeted 30 m/s. The pressure drops were within limits of the targeted 10 kPa (gas) and 70 kPa (water).

The primary data assumed for design are projected in Table 2. Further data which were obtained from design handbooks for calculations are projected in Tables 3 and 4. Using the drawings from software and the iterations, finalised geometric data are projected in Table 5. Figures 8, 9 and 10 shows the arrangement of the new design. Figure 11 shows the comparison of the existing and the new designs.

Comparison

Referring to Table 5 and Fig. 11, the features of the new design may be compared. The number of tubes has increased nearly six times but the effective length has been reduced. The number of tubes was accommodated in the shell keeping the requirements of tube count data referred to by Perry [18].

In the existing design, the area required is complemented by the fins fitted on the tubes. In the new design, tube surface alone forms the heat transfer area with a reduction of 22–23 % from existing area. The tube diameter has been increased and arranged to handle the gas whereas in the existing design, water flows through the tubes. The increased size will facilitate better cleaning of the tubes.

The new tube thickness is half of the existing design resulting in improved heat transfer coefficient. The tube

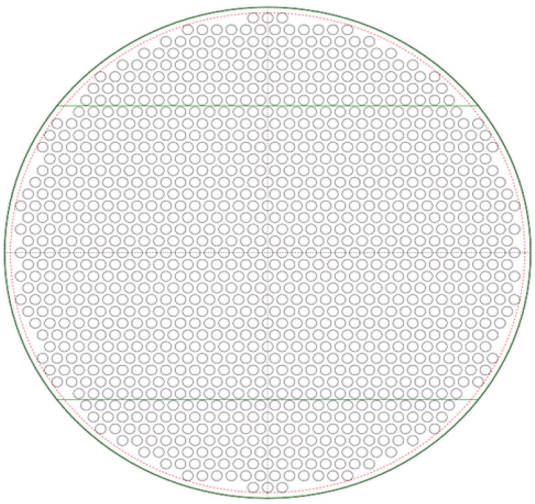

Fig. 8 Tube arrangement of new design

length to shell diameter ratio is 0.98–1 limiting the length of the heat exchanger. The reduction in tube length and area will improve the vibration characteristics. The nozzle sizes were slightly increased for the shell and tube design to avoid the backpressure on turbochargers and the circulating pumps.

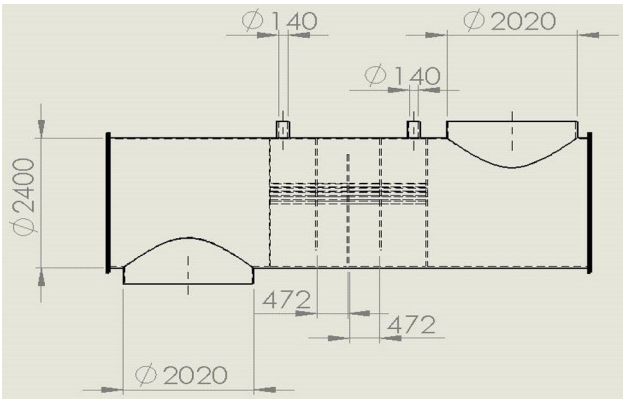

Fig. 9 Principal dimensions of new design

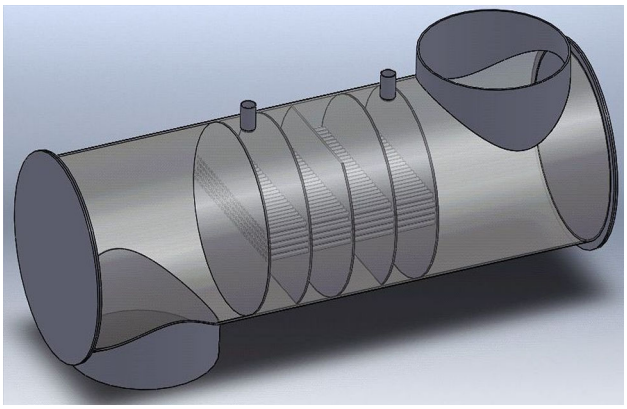

Fig. 10 Visualisation of the new design

The extreme shell dimension worked to almost twice the extreme length of existing design. This implies that the location of the new heat exchanger has to be horizontal, either in the athwart ship or longitudinal direction. The space availability for this was confirmed with the ship's drawings.

Of the non-comparable features, baffles were chosen for an ideal support of the bundle with 20 % cut. The baffle pitch was fixed at the prescribed 1/5 of the shell inside diameter. This optimised design aimed to reduce the leakages in the bypass streams.

Energy lost in exhaust gases of a diesel engine could vary from 25 to 40 % of the input energy [20, 21]. Present day research efforts in harvesting the waste heat from exhaust gases focus on reducing emissions and improving efficiency [22]. A well-designed heat exchanger is imperative for realising these objectives. Considering the recovery functions and heat duty, the shell and tube redesign appears viable. Designing methods based on known economic and technical parameters have been demonstrated earlier [23]. In the current study, the new design fares better in terms of simplicity of construction, lesser heat transfer area and pressure drop.

Conclusions

In comparison with processing industry applications, shipboard resources are limited. So, marine applications require designs with lesser excessive margins. On similar lines, designs have been worked using values obtained from software drawings. An approach involving theoretical calculations and engineering software has been demonstrated with this study considering such factors.

Acknowledgments The author is thankful to MISC Berhad for the information and data on shipboard heat exchangers.

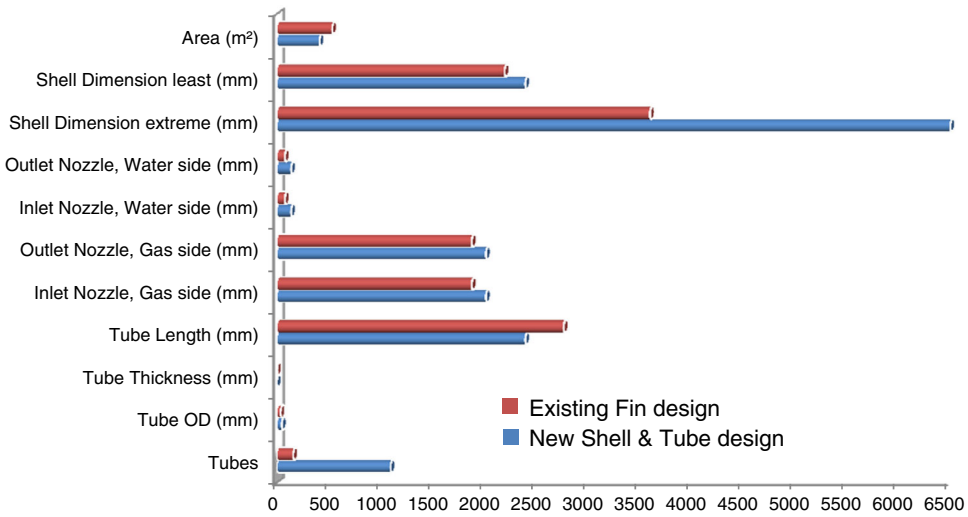

Fig. 11 Comparison of new and existing designs

Appendix

See Tables 6 and 7.

Table 6 Design calculations: heat transfer coefficient

Equations	Sub equations/attained values	Remarks/geometric dimensions
Heat transfer coefficient, tube side		
$\alpha_i = \frac{\lambda_t}{d_h} Nu_t = 109.4$	$Nu_t = \frac{Re_t Pr_t \xi/8}{1+12.7\sqrt{\xi/8}(Pr_t^{2/3}-1)}\left[1+\left(\frac{d_h}{L}\right)^{2/3}\right] = 132$	d_h =0.464 (hydraulic diameter = inside diameter)
	Fully developed turbulent flow for $0.5 < Pr_t < 2{,}000$ and $3{,}000 < Re_t < 1{,}000{,}000$	
	Friction Factor $\xi = (0.78\, ln\, Re_t - 1.5)^{-2}$	
	$Re_t = \frac{\rho_t w_t d_h}{\eta_t} = 60776$	Eqs. (12, 13, 14)
	$Re_t > 10{,}000$, with turbulent flow	
Heat transfer coefficient, shell side		
$\alpha_o = \frac{\lambda_s}{l'} Nu_s = 699.1$	$\alpha_o = \frac{\lambda_s}{(\pi/2)d_o} Nu_s$	$d_o = 0.05$ (outside diameter)
	l' is taken as $(\pi.d_o/2)$	
	$Nu_s = f_w Nu_b = 77.75$	(Eqs. 16, 17, 18, 19, 20)
	$f_w = f_g f_l f_b$	
	$= 1.079 \times 0.7766 \times 0.9161$	
	$= 0.7679$	
	$Nu_b = f_n f_p Nu_{ib} = 101.2$	
	$f_n = 1$ factor for effect of tube rows	
	$Nu_{ib} = f_a Nu_{cb}$	
	$Nu_{cb} = 0.3 + \sqrt{Nu_{laminar}^2 + Nu_{turbulent}^2} = 63.59$	(Eqs. 21,22, 23, 24, 25)
	$Nu_{laminar} = 0.664\sqrt{Re_{\psi l}} \cdot \sqrt[3]{Pr} = 52.22$	$D_i = 2360$; $S = 472$
	$Re_{\psi l} = \frac{w l'}{\psi \nu} = 4494$	$S_1 = 65$; $S_2 = 56.29$
	$w = \frac{\dot{V}}{A_f}$	
	A_f is product of inside diameter of the shell and the baffle spacing	
	Void fraction	
	$\psi = 1 - \pi/4ab$ if $b \geq 1$or $1 - \pi/4a$ if $b < 1$,	
	where $a = \frac{S_1}{d_o}$ and $b = \frac{S_2}{d_o}$	
	$Nu_{turbulent} = \frac{0.037 Re_{\psi l}^{0.8} Pr}{1+2.443 Re_{\psi l}^{-0.1}\left(Pr^{\frac{2}{3}}-1\right)} = 35.76$	(Eqs. 23, 26, 27, 28)
	$f_a = 1 + \frac{2}{3b} = 1.592$	
	Arrangement factor	
	Correction factor for change of physical properties in fluid flow	
	$f_p = \left(\frac{Pr}{Pr_w}\right)^{0.25} = 1.029$	
	Geometry correction factor	
	$f_g = 1 - R_G + 0.524\, R_G^{0,32} = 1.079$	
	Leakage correction factor	$e = 15$; $e_1 = 50$
	$f_l = 0.4\frac{A_{gtb}}{A_{sg}} + \left(1 - 0.4\frac{A_{gtb}}{A_{sg}}\right)\exp(-1.5R_L) = 0.7766$	$L_E = 610$
	$A_{sg} = A_{gtb} + A_{gsb} = 0.07613$	$d_b = 50.8$
	$A_{gtb} = \left(N_t + \frac{n_w}{2}\right)\frac{\pi\left(d_b^2 - d_o^2\right)}{4} = 0.06048$	$n_w = 288$
	$A_{gsb} = \frac{\pi}{4}\left(D_i^2 - D_{baf}^2\right)\frac{360-\gamma}{360} = 0.01565$	$\gamma = 106.4°$
	$\gamma = 2\cos^{-1}\left(1 - \frac{2H}{D_{baf}}\right)$	(Eqs. 29, 30, 31, 32, 33, 34, 35)
	$R_L = \frac{A_{sg}}{A_e}$	
	$A_e = S \cdot L_E$	
	$L_E = 2e_1 + \sum e$	

Geometric data required: Shell inside diameter, Tube bundle diameter (Diameter of Circle touching all the outermost tubes), Baffle diameter, Outer diameter of tubes, Baffle hole diameter, Height of baffle cut, Baffle spacing, Transverse and longitudinal pitch, Sum of shortest connections, Number of tubes, Tube arrangement (staggered/in-line), Number of tubes in upper/lower window sections, Number of main resistances

Table 7 Design calculations: pressure drops

Equations	Sub equations/attained values	Remarks/geometric dimensions
Pressure drop, tube side		
$\Delta p_{tube} = \Delta p_n + \Delta p_{e\ in\ out} + \Delta p_{friction} = 1{,}488$	$\Delta p_n = \Delta p_{in\ noz} + \Delta p_{out\ noz} = 168.4 + 154.5$	$D_{noz\ in} = 1{,}998$ (Inlet nozzle inside diameter)
	Pressure drop in the nozzle sections	(Eqs. 43, 44, 45, 46)
	$\Delta p_{noz} = \frac{\xi \cdot \rho}{2w^2_{nozzle}}$	
	$w_{nozzle} = \frac{4m_t}{\pi \cdot D^2_{noz\ in} \cdot \rho_{noz}}$	
	Pressure drop in the inlet and outlet sections	K_e assumed 0.9
	$\Delta p_{e\ in\ out} = K_e \frac{\rho_t w_t^2}{2}$	(Eqs. 47, 48)
	$w_t = \frac{4m_t}{d_i^2 \cdot \rho_t \cdot N_t}$	
	Pressure drop due to friction	Φ, Ψ assumed to be unity
	$\Delta p_{friction} = \Delta p_{tube\ friction} \cdot F_t$	(Eqs. 49, 50, 51)
	$\Delta p_{tube\ friction} = 2\xi_{tube} \frac{\rho_t \cdot w_t^2 \cdot NTP \cdot L}{d_i}$	
	$\xi_{tube} = \xi_{tubein} \cdot \Phi \cdot \Psi$	
Pressure drop, shell side		
$\Delta p_{shell} = (N_b - 1)\Delta p_q + 2\Delta p_{qe} + N_b \Delta p_w + \Delta p_n = 304.6$	Pressure drop in central section	$N_b = 3$
	$\Delta p_q = \Delta p_{qo} f_L f_B = 1.858$	$n_{mr} = 25$
	$\Delta p_{qo} = \xi_{stb} \cdot n_{mr} \cdot \frac{\rho_s w_e^2}{2} = 4.775$	(Eqs. 55, 56, 57, 58)
	$w_e = \frac{\dot{V}}{A_e}$	
	$\xi_{stb} = \xi_{lam} \cdot f_{zl} + \xi_{turb} \cdot f_{zt}\left[1 - exp\left(-\frac{Re_{s1}+200}{1000}\right)\right] = 0.6858$	(Eqs. 59, 60, 61, 62, 63, 64, 65, 66)
	$f_{alv} = \frac{280\pi\left[\left(b^{0.5}-0.6\right)^2+0.75\right]}{(4ab-\pi)a^{1.6}} = 205.1$	
	$f_{atv} = 2.5 + \left(\frac{1.2}{(a-0.85)^{1.08}}\right) + 0.4\left(\frac{b}{a} - 1\right)^3 = 5.342$	
	$Re_{s1} = \frac{w_e\ d_o\ \rho_{sm}}{\eta_{sm}}$	
	$f_{zl} = \left(\frac{\eta_w}{\eta_{s\,m}}\right)^{\frac{0.57}{\left[\left(\frac{4ab}{\pi}-1\right)Re_{s1}\right]^{0.25}}} = 0.9917$	
	$f_{zt} = \left(\frac{\eta_w}{\eta_{sm}}\right)^{0.14} = 0.984$	
	$\xi_{lam} = \frac{f_{alv}}{Re_{s1}} = 0.04682$	
	$\xi_{turb} = \frac{f_{atv}}{(Re_{s1})^{0.25}} = 0.6565$	
	Leakage correction factor	(Eq. 67)
	$f_L = exp\left[-1.33(1 + R_M)R_L^r\right] = 0.4948$	
	$r = [-0.15(1 + R_M) + 0.8]$	
	$R_M = \frac{A_{gsb}}{A_{sg}} = 0.2055$	
	Bypass correction factor	(Eqs. 68, 69, 70)
	$f_B = exp\left[-\beta R_B\left(1 - \sqrt[3]{2R_S}\right)\right] = 0.7866$	
	$R_B = \frac{A_b}{A_c} = 0.06489$	
	$R_S = \frac{n_s}{n_{mr}} = 0$ (no sealing strips)	
	Pressure drop in end sections	(Eqs. 71, 72) $S_e = 492$
	$\Delta p_{qe} = \Delta p_{qe0} \cdot f_B = 4.612$	
	$\Delta p_{qe0} = \xi_{stb} \cdot n_{mre} \cdot \frac{\rho_s w_{ez}^2}{2} = 5.863$	
	$w_{ee} = \frac{\dot{V}}{A_{ee}} = w_e \frac{S}{S_e} = 0.02314$	
	Pressure drop in window section	(Eq. 75)
	$\Delta p_w = \sqrt{\Delta p^2_{w\ lam} + \Delta p^2_{w\ turb}} f_Z f_L = 0.7328$	
	$\Delta p_{w\ lam} = \left[\frac{56}{\left(\frac{w_z \rho_s e}{\eta_{sm}}\right)} n_{mrw} + \frac{52}{\left(\frac{d_g\ w_z\ \rho_s}{\eta_{sm}}\right)}\left(\frac{S}{d_g}\right) + 2\right]\left(\frac{\rho_s w_z^2}{2}\right) = 0.5594$	(Eqs. 76, 78, 79, 80, 81)
	$n_{mrw} = 0.8H/s_2$	$H = 472$
	$d_g = \frac{4A_w}{U_w} = 55.74$	$D_{baf} = 2{,}354$
	$A_w = A_{wt} - A_t$	
	$A_{wt} = \frac{\pi}{4} D_i^2 \left(\frac{\gamma}{360}\right) - \frac{\left(D_{baf} - 2H\right)D_{baf}}{4} \cdot sin\left(\frac{\gamma}{2}\right)$	
	$U_w = \pi D_i \left(\frac{\gamma}{360}\right) + \pi d_o \left(\frac{n_w}{2}\right)$	
	$\Delta p_{w\ turb} = (0.6n_{mrw} + 2)\left(\frac{\rho_s w_z^2}{2}\right) = 1.397$	(Eqs. 77, 82)
	$w_z = \sqrt{(w_e w_p)}$	
	$w_p = \dot{V}/A_w$	
	$\Delta p_n = \xi_{noz} \frac{\rho_s w_n^2}{2} = 286.8$	(Eqs. 83, 84)
	$w_n = \frac{\dot{V}}{\frac{\pi}{4} d_n^2}$	

Geometric data required: Shell inside diameter, Tube bundle diameter (Diameter of Circle touching all the outermost tubes), Baffle diameter, Outer diameter of tubes, Baffle hole diameter, Height of baffle cut, Baffle spacing, Transverse and longitudinal pitch, Sum of shortest connections, Number of tubes, Tube arrangement (staggered/in-line), Number of tubes in upper/lower window sections, Number of main resistances, Nozzle diameters, Number of baffles

References

1. T. Kuppan, *Heat Exchanger Design Handbook* (Marcel Dekker Inc., New York, 2000), p. 2
2. M.A.S.S. Ravagnani, J.A. Caballero, A MINLP model for the rigorous design of shell and tube heat exchangers using the TEMA standards, Institution of Chemical Engineers, Chemical Engineering Research and Design. Trans. IChem. E **85A**(10), 1423–1435 (2007)
3. M.C. Tayal, F. Yan, U.M. Diwekar, Optimisation of heat exchangers: a genetic algorithm framework. Ind. Eng. Chem. Res. **38**, 456–467 (1999)
4. G.N. Xie, B. Sunden, Q.W. Wang, Optimisation of compact heat exchangers by a genetic algorithm. Appl. Therm. Eng. **28**, 895–906 (2008)
5. N.M. Khalfe, S.K. Lahiri, S.K. Wadhwa, Simulated annealing technique to design minimum cost heat exchanger. Chem. Ind. Chem. Eng. Q. **17**(4), 409–427 (2011)
6. A.V. Azad, M. Amidpour, Economic optimisation of shell and tube heat exchanger based on constructal theory. Energy (2010). doi:10.1016/j.energy.2010.11.041
7. A.C. Caputo, P.M. Pelagagge, P. Salini, Heat exchanger design based on economic optimisation. Appl. Therm. Eng. **28**, 1151–1159 (2008)
8. A.L.H. Costa, E.M. Queiroz, Design optimisation of shell and tube heat exchangers. Appl. Therm. Eng. **28**, 1798–1805 (2008)
9. M.S. Peters, K.D. Timmerhaus, R.E. West, *Plant design and economics for chemical engineers*, 5th edn. (McGraw Hill Companies, New York, 2003)
10. K.J. Bell, Heat exchanger design for the process industries. J. Heat Transf. **126**, 877–885 (2004)
11. R. Mukherjee, Effectively design shell and tube heat exchangers, Chemical Engineering Progress, American Institute of Chemical Engineers (1998)
12. TEMA Standards, Tubular Exchangers manufacturers Association, 9th edn. (New York, USA, 2007)
13. J.H. Lienhard IV, *J.H. Lienhard V,A Heat Transfer Textbook*, 4th edn. (Phlogiston Press, Cambridge, Massachusetts, 2011)
14. G.F. Hewitt, G.L. Shires, T.R. Bott, *Process Heat Transfer* (CRC Press, Boca Raton, FL, 1994), pp. 73–79
15. VDI Heat Atlas, 2nd edn. (Springer, Berlin, 2010)
16. M. Serna, A. Jiménez, A compact formulation of the Bell-Delaware design for heat exchanger design and optimisation. Trans. IChem. E **83A**(5), 539–550 (2005)
17. J.P. Holman, *Heat Transfer* (McGraw Hill, New York, 2002)
18. R.H. Perry, D.W. Green, J.O. Maloney, (Editors), Perry's Chemical Engineers' handbook, International Edition, 7th edn. (The McGraw-Hill Companies Inc., 1997)
19. J.M. Coulson, J.F. Richardson, *Chemical Engineering*, vol. 1, 2nd edn. (Pergamon, New York, 1993), p. 577
20. N.M. Al Najem, J.M. Diab, Energy-exergy analysis of a diesel engine. Heat Recovery Syst. CHP **12**(6), 525–529 (1992)
21. D.F. Woodyard (ed.), Theory and general principles, in *Pounder's Marine Diesel Engines and Gas Turbines*, 8th edn. (Elsevier Butterworth Heinemann, Burlington, 2004), p. 6
22. MAN B&W, Waste heat recovery system (WHRS) for reduction of fuel consumption, emissions and EEDI (2012)
23. I. Teke, O. Ağra, O. Atayilmaz, H. Demir, Determining the best type of heat exchangers for heat recovery. Appl. Therm. Eng. **30**, 577–583 (2010)